Time-Domain Characterization of Acoustic Liner Response from Experimental Data Part 1: Linear Response

Laurence R. Keefe* and Patrick H. Reisenthel†
Nielsen Engineering & Research, Mountain View, CA 94043-2241

A time-domain method for characterization of locally reacting acoustic liners from data is described. The procedure yields a compact, ordinary-differential-equation description of liner velocity response to forcing pressure. This description can be linear or weakly nonlinear, depending upon the kind of experimental data input to the method. Such continuous differential equations can be used as boundary conditions in a computational aeroacoustics simulation, and discretized and advanced in time in any fashion consistent with the underlying numerical simulation. Liner dynamics are modeled by a two-term Volterra integral expansion. Experimental response data are subsequently used to build robust time-domain models of the kernels in these integrals. Projection of these kernels onto particular classes of analytic forms automatically connects each integral term in the Volterra expansion to an equivalent system of ordinary differential equations. The linear term in the Volterra series is formally equivalent to the frequency-domain impedance description presently used to describe liners. Such impedance data are used in this paper to construct the linear response kernel and the characterizing linear differential equation of two existing liners. In a later paper we describe the method's extension to nonlinear kernel extraction and differential equation projection.

Nomenclature

A	Coefficient matrix in kernel extraction linear system
B	Time constant matrix in the linear kernel matrix representation
C	Solution vector in kernel extraction linear system
CAA	Computational Aeroacoustics
D_j^i	Coefficients in inhomogeneous, single differential equation description of liner response
K_i	i^{th}-order Volterra kernel
M	Excitation matrix in kernel extraction least-squares linear system
ODE	Ordinary differential equation
OLJ	Özyöruk-Long-Jones (Reference 6)
$P(\omega)$	Fourier transform of pressure at the liner surface
$R(\omega)$	Resistance
SVD	Singular Value Decomposition
V	Data vector in kernel extraction linear system
$V(\omega)$	Fourier transform of normal velocity at the liner surface
W	Data vector in kernel extraction least-squares linear system
$X(\omega)$	Reactance
$Z(\omega)$	Acoustic liner impedance ($Z(\omega) = P(\omega)/V(\omega)$)

*Senior Research Scientist, 605 Ellis St., Senior Member

†Chief Scientist, 605 Ellis St., Senior Member

Z_i	Complex time constant in linear kernel expansion
c_0	Speed of sound
c_n	Expansion coefficients in linear real kernel representation/basis function coefficients
f	Frequency
i	Complex pure imaginary (i^2 = -1)
p(t)	Input pressure signal
r	Inhomogeneous coefficient vector multiplying pressure in equivalent linear ODE system
t	Time
v(t)	Output acoustic velocity, = $v_1 + v_2$
v_1	Linear acoustic velocity
v_2	Second-order acoustic velocity
w_i	Auxiliary dynamic variable in equivalent linear ODE system
x	System input
y	Total system output
y_i	Component of system output
$\mu_i(t)$	Kernel extraction basis functions
ρ_0	Mean fluid density
τ_i	Auxiliary time integration variable
ω	Angular frequency
Π_j^i	Coefficients in inhomogeneous, single differential equation description of liner response

I. Introduction

Suppression of jet engine noise by inlet and exhaust duct liners is an important part of developing environmentally acceptable aircraft. Because methods for transfer of frequency-domain impedance data to linear time-domain boundary conditions are still under development, Computational Aeroacoustics (CAA) is not used widely to design new liners or predict preinstallation performance of existing ones. Also, the methods that do exist are not easily extended to cover finite amplitude effects due to high sound pressure levels or liner material nonlinearities. This paper describes a two-step application of Volterra (integral) series methods to produce a weakly nonlinear, time-domain characterization of liners. The two steps in the method are (1) robust time-domain modeling of the integrals that make up the Volterra representation of liner response to pressure fluctuations, and (2) conversion of this integral representation into an equivalent time-domain, nonlinear differential equation description of the liner dynamics. Applying this modeling technique to liner response data results in forced, time-domain, differential equations for liner velocity response to the acoustic pressure. The differential equations can be linear or nonlinear. Linear equations are generated from existing frequency-domain liner impedance data, whereas nonlinear equations require new time-domain acoustic measurement techniques. The resulting equations can be rapidly integrated and discretized in any fashion consistent with the CAA calculation where they are used.

The basis of the liner characterization scheme is the Volterra-Wiener theory of nonlinear systems[1,2] which states that, under general conditions, a nonlinear, causal, time-invariant system may be represented exactly as an infinite series of multidimensional integrals

$$y(t) = \sum_{n=1}^{\infty} y_n(t) = \sum_{n=1}^{\infty} \int_0^t \cdots \int_0^t K_n(t-\tau_1, t-\tau_2, \cdots, t-\tau_n)\, x(\tau_1) \cdots x(\tau_n)\, d\tau_1 \cdots d\tau_n \tag{1}$$

This may be regarded as an alternative to the more familiar differential equation description of an input-output system.

$$f\left(x, \frac{dx}{dt}, \frac{d^2x}{dt^2}, \ldots \frac{d^M x}{dt^M}; y, \frac{dy}{dt}, \frac{d^2y}{dt^2}, \ldots \frac{d^N y}{dt^N}\right) = 0 \tag{2}$$

The point of view adopted here is that of a locally reacting acoustic liner treated as a black box, with input x(t) and output y(t). y(t) is the macroscopic normal velocity at the wall, and x(t) is the amplitude of the pressure, which acts as the excitation (see Fig. 1). The term K_n is the n^{th}-order Volterra kernel.

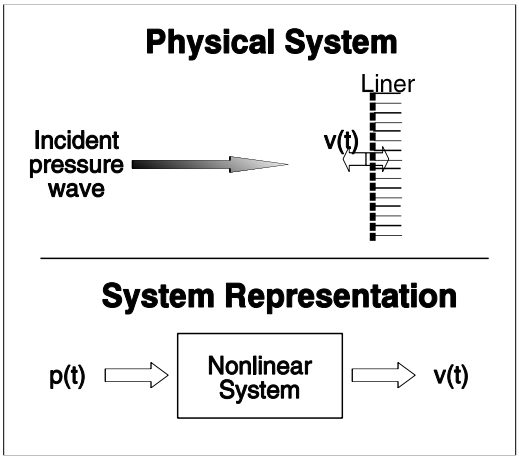

Figure 1. System Representation

The Volterra series approach derives from the large body of work carried out in connection with the modeling of nonlinear systems "with memory."[3] Volterra theory has a solid mathematical foundation and is the topic of many texts.[4] However, Equation (1) is formidable, and, typically, only a few terms are retained (truncated Volterra series). For example, the first term in the series is

$$y_1(t) = \int_0^t K_1(t-\tau_1)x(\tau_1)\,d\tau_1 \tag{3}$$

This term is the Duhamel, or impulse response, integral of linear systems theory. The second, third, and higher-order terms describe nonlinear effects dependent on amplitude and system memory. Thus, if the liner velocity response to pressure is strictly linear,

$$v(t) = \int_0^t K_1(t-\tau_1)p(\tau_1)\,d\tau_1 \tag{4}$$

Equation (4) is a convolution integral which involves only the knowledge of the excitation time history p(t) and the first-order kernel K_1. The latter is the *unit impulse response* of the system, i.e., the temporal response of the system to a Dirac delta function. Equation (4) is the time-domain equivalent of a *linear transfer function* representation, i.e., using capitalized letters to denote Fourier-transformed variables and ω as the frequency:

$$V(\omega) = K_1(\omega)P(\omega) \tag{5}$$

In other words, if Z is the impedance, $K_1(\omega) = 1/Z$.

Previous works[5,6,7] on linear time-domain liner characterization have begun with Eq. (5). The idea is simple: given experimentally derived or modeled spectral impedance data (Eq. (5)), simply inverse Fourier transform to obtain the appropriate time-domain equation. The basic difficulty encountered with this method is that of insuring stability and causality when inverting the transform, and this was recognized as a general problem. In Ref. 7 Fung and Ju suggested that inversion of the velocity reflection coefficient, instead of impedance, avoids stability problems, and proceeded to develop models for this coefficient which yield reflection impulse response functions in the time domain that are sums of damped trigonometric functions. This conversion of the frequency-domain information into a time-domain convolution integral is equivalent to the first step in the process described here. However, these authors stopped at this step, and implemented a numerical evaluation of the convolution integral in their CAA code instead of converting it to a differential equation, as is done here. General forms of the impedance/reflection relation

are talked about in these papers, but quite simple models are postulated in the end so that the inverse transform is obtainable. This has been valuable work, but it does not generalize to include nonlinear effects. In addition, its exclusion of higher-order impedance/reflection models to avoid analytical difficulties ignores the realities of current experimental data and the expected response characteristics of multilevel liners. In Ref. 6, Özyöruk, Long, and Jones (OLJ) perform a rational function fit to ceramic liner impedance data, and then use properties of the Z-transform to produce a discrete inverse that yields time-domain liner behavior directly, without an intervening differential equation. In a later paper Ju and Fung[8] model the reflection kernel for the OLJ data as a single, phase-shifted, damped sinusoid. An analysis of the OLJ data in this work shows the kernel to be better described by the sum of two such functions. The difference in the number of basis functions in the kernel occurs because Ju and Fung assume a model, whereas the current method is blind, and finds the kernel model that gives the best system identification. Previous work on nonlinear time-domain characterization is restricted to the pioneering work of Zorumski and Parrot.[9] From data, this method produces equations relating acoustic resistance and reactance to empirically determined nonlinear functions of the velocity. However, the results are not in a form convenient for use in simulations. In addition, the nonlinear impedance idea has built-in conceptual difficulties; impedance is defined at a single frequency, yet multiple-frequency response to single-frequency input is a hallmark of nonlinear dynamics.

Since analytic, first-principles calculations of the full, locally reacting, nonlinear relation between liner acoustic velocity and pressure are generally not available, all approaches to liner characterization, including the one described here, employ models of that response. Frequency-domain techniques developed so far are inherently linear, and must select models in that domain that ensure causality and well-posedness upon inversion. Nonlinear frequency-domain liner response modeling is possible,[10] but the data requirements are strenuous and problems upon inversion are compounded. Modeling directly in the time domain, the current technique avoids inversion problems, and extends simply to include nonlinear effects.

In the following the theoretical basis for time-domain kernel extraction is established first, and then followed by a similar section describing kernel projection onto equivalent differential equation models. This theory is then applied to data from both a ceramic tube and conventional perforate liner to obtain their time-domain differential equation description. This paper primarily covers the linear aspects of kernel extraction and projection. The theory for weakly nonlinear extensions of these processes has been worked out already,[11] but is sufficiently complicated, particularly in the case of kernel projection, to merit a separate description at a later time. These results are briefly stated, but not explained.

II. Truncated Volterra Series Modeling of Liner Response

Although the convergence of the full Volterra series model, Eq. (1), is guaranteed, the utility of such descriptions is usually judged by their ability to produce a good approximation of the full series behavior from a few, lower-order terms. At low sound pressure levels there is extensive experience to indicate that liner behavior is well approximated by the first term in the expansion. As an approximate extension to describe weakly nonlinear effects at higher sound levels, it is natural to assume a two-term truncation of the Volterra series. Thus

$$v(t) \approx v_1(t) + v_2(t) \tag{6}$$

with

$$v_1(t) = \int_0^t K_1(t-\tau_1)p(\tau_1)\,d\tau_1 \tag{7}$$

and

$$v_2(t) = \int_0^t\int_0^t K_2(t-\tau_1, t-\tau_2)p(\tau_1)p(\tau_2)\,d\tau_1 d\tau_2 \tag{8}$$

The first step in the liner characterization procedure is to develop robust time-domain models of the kernels in each integral in the truncated series. This is achieved by expanding the unknown kernels in some basis function space $\{\mu_j(t)\}$, and calculating the expansion coefficients that yield the best fit. Thus for the linear kernel assume

$$K_1(t) = \sum_j c_j \mu_j(t) \tag{9}$$

and substitute in Eq. (7) to obtain

$$v_1(t) = \sum_j c_j \int^t \mu_j(t-\tau_1)\, p(\tau_1)\, d\tau_1 \tag{10}$$

Equation (10) is regarded as a constraint which the c_j basis coefficients must satisfy at all times. Thus, to solve for n coefficients, c_1 through c_n, one must construct at least n independent realizations of Eq. (10). This requires n different simultaneous time histories of the pressure and velocity at the liner's surface. Each realization yields an equation of the type

$$v_1(t_i) = \sum_j c_j \int^{t_i} \mu_j(t_i-\tau_1)\, p(\tau_1)\, d\tau_1 \qquad or \qquad v_1(t_i) = \sum_j c_j a_{ij} \tag{11}$$

The coefficients a_{ij} can be calculated using any integration method, since the input $p(t)$ is known, and so are the basis functions, $\mu_j(t)$. The question of how to *choose* the basis functions is key to the method's success. The particular basis set used in this study consisted of multiresolution Gaussians, and is discussed at length in Refs. 12 and 13. They are versatile and easy to implement, permitting the representation of fairly arbitrary shapes and, therefore, the identification of a large class of impulse response kernels. They are not conducive, however, to the automatic derivation of simple differential equations. Thus, the use of the multiresolution basis functions in this study was only an intermediate step allowing a more accurate determination of the underlying kernel. Once this kernel was identified with sufficient certainty (i.e., the identified kernel is robust with respect to perturbations in the parameters of the extraction), then the next step was to fit the kernel with basis functions that do lend themselves to the derivation of a low-dimensional system of ordinary differential equations (see below). For the remainder of this discussion, it can be assumed that the $\{\mu_j(t)\}$ basis functions are known and form a complete set. The main point to be made here is that each realization described by Eq. (11) represents one row in a matrix system. The basic principle behind the extraction procedure is that, through multiple instances of the hypothesized truncated Volterra series model, one ends up formulating a linear system of equations

$$[A][C] = [V] \tag{12}$$

where $A \equiv [a_{ij}]$ is the excitation matrix, $[V]$ represents the measured velocity data, and $C = [c_1, c_2, \cdots, c_n]^T$ is the solution vector.

Equation (12) is fundamental to the extraction method. The same equation is obtained whether one is solving for 200 numerical samples of the Volterra kernel, or, say, three coefficients in a judiciously chosen basis function expansion (Jacobi polynomials, Laguerre functions, and the like), or coefficients of bi-orthogonal wavelets in a multiresolution signal decomposition of the unknown kernel.[13] Most importantly, the same fundamental equation is also obtained in the *nonlinear case* when identifying higher-order kernels. For example, using only the first two terms in a nonlinear Volterra series expansion,

$$v(t) = \int^t K_1(t-\tau_1)\, p(\tau_1)\, d\tau_1 + \int^t\!\!\int^t K_2(t-\tau_1, t-\tau_2)\, p(\tau_1) p(\tau_2)\, d\tau_1 d\tau_2 + \ldots \tag{13}$$

and expanding the kernels in an appropriate basis set:

$$K_1(t_1) = \sum_j c_j^{(1)} \mu_j^{(1)}(t_1) \ , \quad K_2(t_1,t_2) = \sum_k c_k^{(2)} \mu_k^{(2)}(t_1,t_2) \ , \quad \ldots \tag{14}$$

it follows that

$$\begin{aligned} v(t_i) &= \sum_j c_j^{(1)} \int^{t_i} \mu_j^{(1)}(t_i - \tau_1)\, p(\tau_1)\, d\tau_1 \\ &+ \sum_k c_k^{(2)} \int^{t_i}\int^{t_i} \mu_k^{(2)}(t_i - \tau_1, t_i - \tau_2)\, p(\tau_1) p(\tau_2)\, d\tau_1 d\tau_2 \ + \ \ldots \end{aligned} \tag{15}$$

or:

$$v(t_i) = \sum_j c_j^{(1)} a_{ij}^{(1)} + \sum_k c_k^{(2)} a_{ik}^{(2)} + \ \ldots \tag{16}$$

The $a_{ij}^{(m)}$ (m = 1, 2, ...) represent m-dimensional integrals which are known terms, once the input, $p(t)$, is known. By in-lining the unknown vectors $\{c_j^{(1)}\}$, $\{c_k^{(2)}\}$, ... , we thus obtain a linear system of equations similar to Eq. (12). This is no surprise, since, although the Volterra series is nonlinear with respect to the excitation, $p(t)$, the various expansions are *linear* with respect to the individual kernels.

The principle difficulty with solving Eq. (12) is that the $[A]$ matrix is frequently singular. This is because the problem of indirect kernel identification (i.e., the inference of the kernels from experimental observations) is, fundamentally, improperly posed. There are two reasons for this. One of them is nonuniqueness: there may be more than one kernel capable of reproducing the limited quantities of data available. For example, it can be shown that, for a single frequency excitation and a linear system, the rank of the $[A]$ matrix is two, regardless of the number of input/output time histories (matrix rows) input as constraints. A second, related reason is simply that the right-hand side, $[V]$, may not satisfy the postulated truncated Volterra series representation.

Both issues (lack of a unique solution, when it exists, or absence of an exact solution) are addressed by considering the solution to $[A][C] = [V]$ in the *least-squares* sense. In other words, we require that the solution vector $[C]$ simultaneously satisfy multiple sets of excitation data $[A^{(m)}][C] = [Y^{(m)}]$ in an approximate sense. Such a condition is expressed by minimization of the modeling error in the least-squares sense, which results in the following matrix equation:

$$\sum_m [A^{(m)T}][A^{(m)}][C] = \sum_m [A^{(m)T}][V] \tag{17}$$

or

$$[M][C] = [W] \tag{18}$$

where $[M]$ is the least-squares excitation matrix and $[W]$ is the least-squares data vector. Note that the linear system, Eq. (18), may still be stiff, and the challenge is to find a "good" solution. Such a solution is obtained by means of a singular value decomposition (SVD) procedure. In the SVD procedure, the linear system $[M][C] = [W]$ is solved by taking the pseudoinverse of $[M]$. This procedure is the topic of many texts,[14,15] and will not be discussed here. In practice, the least-squares and SVD regularization are performed together. The quality of the extraction results depends to a large extent on the quality and quantity of the available data; it is not possible to draw any general conclusions *a priori*. Past experience[12] has shown, however, that the pseudoinverse technique described above is robust and works well with noisy experimental data.

III. Data Requirements for Kernel Extraction

The extraction technique just described works on data in the time domain, rather than the frequency-domain data commonly obtained in impedance measurements. Pulse time histories are the preferred input to the kernel extraction process, since they are frequency rich. This suggests new measurement techniques need to be developed to provide data for this liner characterization method, particularly for its nonlinear extension. However, in the

interim, frequency-domain impedance data will still serve well for strictly linear kernel identification. Synthetic time-domain data were constructed from phase and amplitude data contained in the impedance at a given frequency. If the complex pressure and velocity amplitudes at frequency ω are related by

$$\frac{P}{V} = Z = R + iX \tag{19}$$

then in the time domain

$$Re\{Ve^{-i\omega t}\} = Re\{(P/Z)e^{-i\omega t}\} \tag{20}$$

On the order of two hundred, different, single-frequency time histories of liner pressure and velocity must be substituted into Eq. (11) to obtain $[A]$ matrices of sufficient rank for a robust representation of a liner kernel to be obtained from the least-squares solution technique. These frequencies must cover a range from well below to well above the usual frequencies of maximum liner response, since high frequency behavior controls the short time kernel response, and low frequency behavior controls the long time response. Experimental impedance data rarely provides either the frequency resolution or range required. For this reason an impedance model must be developed from the experimental data to cover the frequency range, so that the necessary number of realizations can be generated easily. These impedance models are discussed separately in Section V, where experimental data are used to generate differential equation descriptions of both a ceramic and perforate liner.

IV. Differential Equation Projection

The modeling assumption embedded in utilizing an impedance description of liner response is that the corresponding differential equation relating acoustic pressure and velocity at the liner surface is linear and constant-coefficient. The homogeneous solutions to such an equation are complex exponentials, or polynomials in time multiplied by complex exponentials if there are repeated roots of the characteristic equation. The response kernel of such a system is naturally described as a linear combination of these functions. Their lack of orthogonality means exponentials are not optimum for general functional approximation problems. However, they are ideal for describing linear kernels derived from constant coefficient equations. For this reason it makes sense to project the extracted kernel derived from liner impedance data onto an unknown linear combination of such functions. Once the system time constants and coefficients in this expansion are identified, the constant coefficient differential equation that is equivalent can be written immediately.

Generally, for any kernel K_1 that may be approximated as a sum of complex exponential basis functions

$$K_1(t) = \sum_{i=1}^{n} c_i e^{-Z_i t}, \qquad (c_i, Z_i) \in \mathbb{C}^2 \tag{21}$$

v(t) must satisfy the following differential equation:

$$\sum_{j=0}^{n} \Pi_j^n \frac{d^{n-j}v}{dt^{n-j}}(t) = \sum_{j=1}^{n} D_j^n \frac{d^{n-j}p}{dt^{n-j}}(t) \tag{22}$$

with these definitions for the fixed coefficients Π_j^n and D_j^n

$$\begin{aligned} \Pi_{j>0}^n &= \sum_{1 \le i_1 < i_2 < \ldots < i_j \le n} Z_{i_1} Z_{i_2} \ldots Z_{i_j}, \qquad \Pi_0^n = 1 \\ D_{j>0}^n &= \sum_{m=1}^{j} \Pi_{m-1}^n \frac{d^{j-m}K_1}{dt^{j-m}}(0) \end{aligned} \tag{23}$$

Thus, the expected differential equation is inhomogeneous, constant-coefficient linear, and of order n (n being the number of exponentials needed to represent the kernel). The inhomogeneous term is a linear combination of derivatives of p(t) up to order (n-1). For a real-valued kernel, the exponentials in the expansion given by Eq. (21) must appear as complex conjugate pairs, or as single real exponentials.

Initially the determination of the expansion coefficients, c_i, and system time constants, Z_i, was handled by a nonlinear optimization procedure that required good initial guesses for convergence. This procedure was inadequate as a general utility for projecting extracted kernels onto an analytic form automatically equivalent to a differential equation. Not only was it slow, but it depended upon guessing both the number of exponentials (system order) as well as their form (real, complex conjugate, secular). For this reason an alternative approach was developed that could be automated as part of a software application which received experimental time histories at one end, performed kernel extraction and projection, and then output the desired differential equation description. These almost automatic system identification methods worked equally well to project the kernels onto Eq. (22) or the more compact differential form:

$$\frac{dw}{dt} = Bw + rp$$
$$v = \sum_{1}^{n} w \tag{24}$$

Here B is a Jordan normal-form matrix of the system time constants, Z_i, and each element of the coefficient vector r is a simple function of the kernel expansion coefficients, c_i. Equations of this form are more conveniently digitized for numerical time advance schemes, and reduce possible precision difficulties associated with Eq. (22).

V. Linear Response Models of Ceramic and Perforate Liners

A. Ceramic Tube Liner

As previously mentioned, the task of identifying the impulse response kernel can be carried out in a fairly systematic manner by using multiresolution pulse basis functions. Because the number of these basis functions can be quite large for general purpose kernels, the identification procedure requires that a similarly large number of realizations be supplied to the method as training data. In the case of the Özyöruk-Long-Jones data, an analytical fit to the impedance data (both resistance and reactance) was available, making it possible to provide response information at both low and high frequencies outside the limited range of the experimental data. The data, shown in Fig. 2, consist of the liner impedance $Z(\omega) \equiv P(\omega)/V(\omega) = R(\omega) + iX(\omega)$, at equally spaced frequencies between 500 Hz and 3 kHz. The curves in the figure are an analytic, low-pass filter model, developed in Ref. 6, that interpolate and extend the data to a wider frequency range.

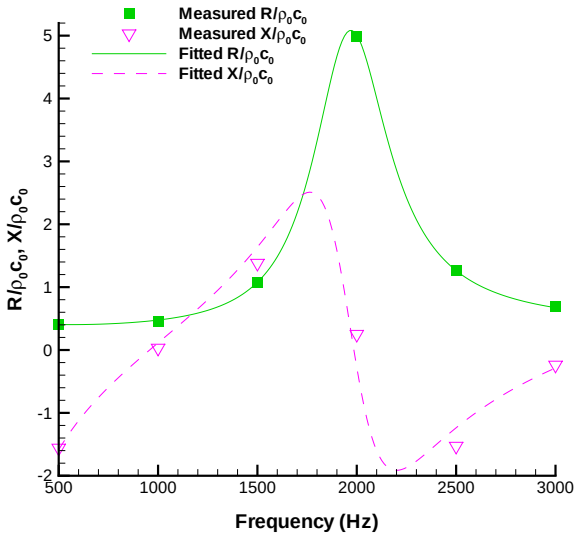

Figure 2 **Frequency-dependent impedance of a constant depth ceramic tubular liner (from Reference [6]).**

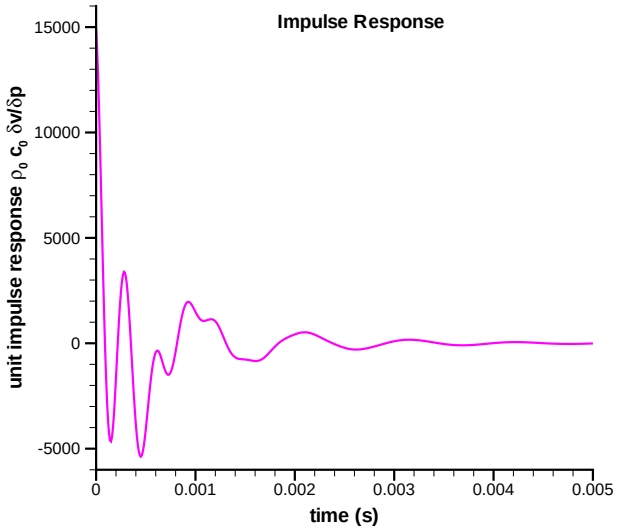

Figure 3 **Extracted unit impulse response corresponding to the Özyöruk-Long-Jones data (Reference [6]).**

Figure 3 displays the linear kernel extracted from these impedance data using synthetic time histories and the least-squares solution technique described in Section II. Its form has been shown to be robust with respect to the number of multiresolution basis functions employed and to differing ensembles of input synthetic time histories. In addition, a Fourier transform of this impulse response is in excellent agreement with the original experimental impedance/admittance data. Note that the impulse response is of v with respect to p, and not p with respect to v. In other words, the training data fed into the extraction scheme was the admittance, $\mathbf{1/Z(\omega)}$, and not the impedance $\mathbf{Z(\omega)}$.

The extracted kernel was projected onto a sum-of-exponentials analytic approximation consistent with the assumption of linear time-invariant liner behavior. Originally this was accomplished with a nonlinear optimization procedure which required good initial guesses on system time constants and a certain amount of operator intervention to converge. The form of the differential equation extracted for this liner's response by this procedure was

$$\frac{d^4v}{dt^4} + 8.132473E{+}03\frac{d^3v}{dt^3} + 4.750106E{+}08\frac{d^2v}{dt^2} + 1.092894E{+}12\frac{dv}{dt} + 1.522664E{+}16v = 1.490175E{+}04\frac{d^3p}{dt^3} + 4.719603E{+}07\frac{d^2p}{dt^2} + 2.278367E{+}12\frac{dp}{dt} + 2.832838E{+}14p \tag{25}$$

As shown in Fig 4, the integration of this fourth-order ODE is functionally equivalent to the calculation of the convolution integral expressed in Eq. (4). This example is relevant to the numerical implementation of the v equation as a boundary condition in a CAA calculation. A step input of pressure excites a wide spectrum of frequencies in the velocity response, yet the integration for long time shows no growth of spurious modes. As should be the case, the velocity response settles to a steady state. Thus the boundary condition itself has no inherent instabilities.

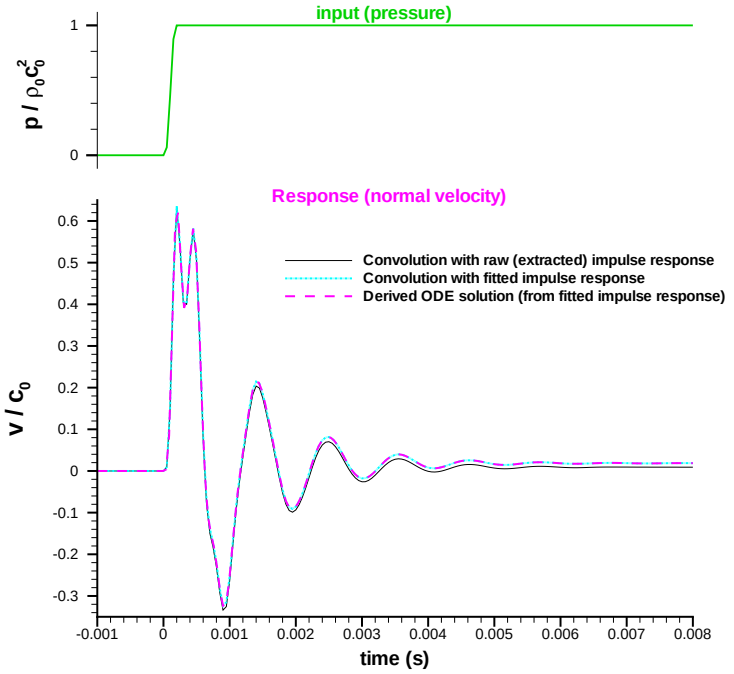

Figure 4 **Predicted normal velocity response to a smooth 7th-order ramp in pressure using three methods: (a) convolution with extracted impulse response, (b) convolution with a four-exponential fit to the extracted kernel, and (c) Runge-Kutta solution of the 4th-order ODE derived from the fit.**

Although this example indicates no difficulty in obtaining reliable results from integrating Eq. (25), note the wide differences in magnitude of the coefficients multiplying the various derivatives of acoustic pressure and velocity. For strictly single-frequency excitation, simple scaling arguments show that these magnitude differences are reduced by the effective factors of $(2\pi f)^k$ implied by the k^{th}-derivative operation. However, at low frequencies, this normalization may be inadequate to overcome the 10^{16} magnitude span of the coefficients on the left-hand side of Eq. (25). A loss in precision is possible in this situation, since even 64-bit arithmetic spans only thirteen orders of magnitude. The compact form expressed by Eq. (24) does not suffer from this same problem. The fourth-order system of ordinary differential equations describing the ceramic liner, and equivalent to Eq. (25), is:

$$\frac{d[w_1, w_2, w_3, w_4]^T}{dt} = \begin{bmatrix} -1026.097 & -5883.723 & 0 & 0 \\ 5883.723 & -1026.097 & 0 & 0 \\ 0 & 0 & -3040.139 & -20435.73 \\ 0 & 0 & 20435.73 & -3040.139 \end{bmatrix} \begin{bmatrix} w_1 \\ w_2 \\ w_3 \\ w_4 \end{bmatrix} + \begin{bmatrix} 1914.781 \\ 2549.001 \\ 4388.395 \\ 6049.570 \end{bmatrix} p \tag{26}$$

$$v = w_1 + w_2 + w_3 + w_4$$

B. Model Perforate Liner

A second test of the liner characterization procedure was performed on a model perforate liner more representative of those currently installed.[16] An analytical fit to the impedance data such as that used for the ceramic liner was not available. Therefore, it was necessary to develop a semiautomatic procedure to fit and extend this, and other, impedance data prior to the creation of synthetic time histories for extraction. The procedure implements analytical extensions to impedance data in both the high- and low-frequency limits, based on prior theoretical work according to which the reactance and resistance are frequency-extrapolated as:

- Reactance:
  - Zero frequency limit: $X(\omega) \propto \mathrm{cotan}(\omega)$
    This is implemented by matching both value and derivative at the lower end of the data interval using the first two terms in a Taylor series expansion of the cotangent.
  - $\omega \to +\infty$ limit: $X(\omega) \propto \omega$
    This is implemented by matching the form $b_1/\omega + b_2\omega$ to the upper end of the data interval (i.e., value and derivative match).
- Resistance:
  - $\omega \to \{0,+\infty\}$ limits: $X(\omega) = const.$
    At low frequencies, this is implemented by matching the form $const + c_2\omega^2$ to the lower end of the data interval.
    At high frequencies, this is implemented by matching the form $const + d_1/\omega + d_2/\omega^2$ to the upper end of the data interval.

For frequency interpolation, i.e., within the data interval, a monotone, shape-preserving spline due to McAllister and Roulier[17] was used, thus providing a globally C^1-continuous representation of the data over the range $\omega \in [0,+\infty($.

The use of the fitting procedure as a preprocessing step is illustrated in Fig. 5 The data are impedance values from a half-scale perforated plate resonator panel with 8.0% porosity. The data shown in Fig. 5 were digitized from Figure (5-4) of Ref. 16. They are the measured resistance and reactance, except for frequencies smaller than 1,500 Hz, where model predictions were used instead. This was done because of acknowledged measurement problems at frequencies below 1,500 Hz. The resulting data and the corresponding analytical fits are indicated in the figure as symbols and lines, respectively.

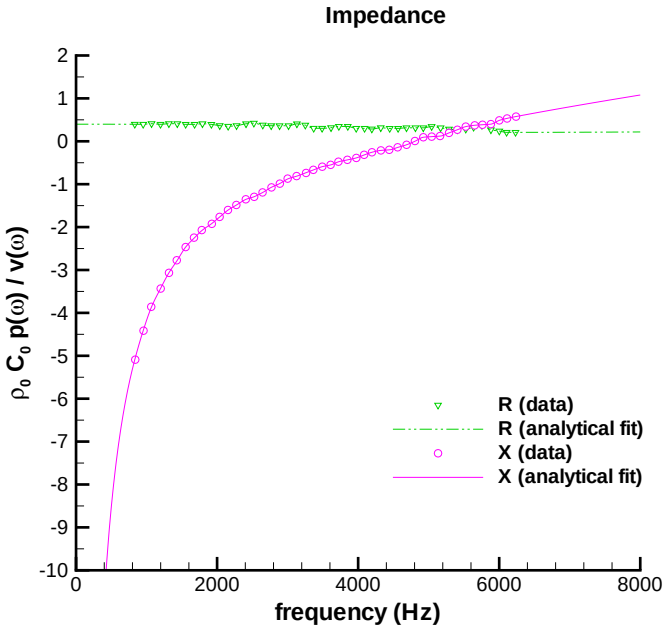

Figure 5. Resistance and Reactance Spectra for a Perforate Liner.

As in the case of the Özyöruk-Long-Jones data, the linear impulse response was extracted using a Gaussian pulse multiresolution basis function set. The resulting first-order Volterra kernel is shown in Fig. 6.

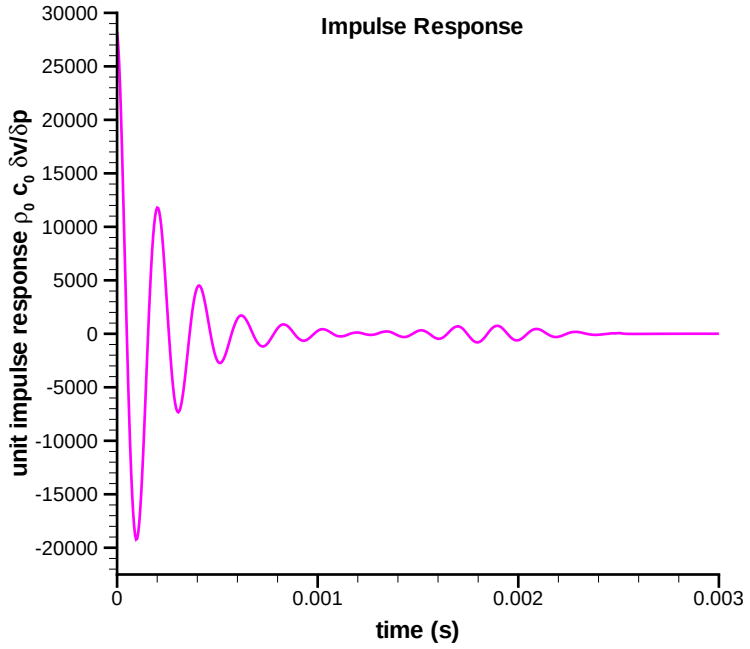

Figure 6. Linear Impulse Response Extracted from Perforate Impedance Data.

The displayed kernel also passed the previously mentioned robustness tests, and showed excellent agreement with the data in Fig. 5 when Fourier transformed. Both the original impedance data and the extracted kernel suggest that the dynamic behavior of this liner is simpler than the ceramic liner. This is confirmed by the extracted differential equation, which is only second-order.

$$\frac{d[w_1, w_2]}{dt} = \begin{bmatrix} -4229.403 & -29684.48 \\ 29684.48 & -4229.403 \end{bmatrix} \begin{bmatrix} w_1 \\ w_2 \end{bmatrix} + \begin{bmatrix} 12427.28 \\ 16237.03 \end{bmatrix} p \tag{27}$$

$$v = w_1 + w_2$$

This system faithfully reproduces the decaying oscillatory behavior of the kernel through the first 1.5 milliseconds, but predicts continuing decay where the extracted kernel shows a brief amplitude increase before the final decay period. It can be shown that a sixteenth-order differential system is required to reproduce this amplitude increase, but it is doubtful that this greater complexity contributes anything significant to the resultant dynamical description of liner behavior.

VI. Conclusions

We describe a method for using data to create a time-domain, differential equation description of an acoustic liner's velocity response to acoustic pressure. Such equations are a compact description particularly suited to use as boundary conditions in computational aeroacoustics simulations, and are more efficient to integrate than equivalent time-domain convolution integrals. These equations may be linear or nonlinear, dependent upon the kind of data supplied. This method works completely in the time-domain and thus avoids difficulties associated with Fourier transforming frequency-domain response data. New experimental methods need to be developed to produce input data suitable for nonlinear equation generation. For linear responding liners, synthetic time history data from measured impedance data serve well for the equation identification procedure. In this case the resulting equations are equivalent to the transfer function description embodied in the use of the impedance concept.

Acknowledgments

This work was supported by NASA Langley Research Center under contracts NAS1-01022 and NAS1-02065. The technical monitor was Dr. Tony Parrott.

References

[1]Volterra, V., *Theory of Functionals and of Integral and Integro-Differential Equations*, Blackie & Sons Ltd., London, 1930.

[2]Wiener, N., *Nonlinear Problems in Random Theory*, Wiley & Sons, Inc., New York, 1958.

[3]Silva, W. A., "A Methodology for Using Nonlinear Aerodynamics in Aeroservoelastic Analysis and Design," AIAA 91-1110, Apr. 1991.

[4]Schetzen, M., "*The Volterra and Wiener Theories of Nonlinear Systems*," Wiley & Sons, New York, 1980.

[5]Tam, C. K. W. and Auriault, L., "Time-Domain Impedance Boundary Conditions for Computational Aeroacoustics," *AIAA Journal,* Vol. 34, No. 5, 1996, pp. 917-923.

[6]Özyöruk, Y., Long, L. N., and Jones, M. G., "Time-Domain Numerical Simulation of a Flow-Impedance Tube," *J. Comp. Phys.*, Vol. 146, 1998, pp. 29-57.

[7]Fung, K-Y and Ju, H. B., "Time Domain Simulation of Acoustics in a Rectangular Duct with Impedance Walls," AIAA-99-1818, 1999.

[8]Ju, H.B. and Fung, K.-Y., "Time-Domain Impedance Boundary Conditions with Mean Flow Effects", AIAA-2000-2003, 2000.

[9]Zorumski, W. E. and Parrott, T. L., "Nonlinear Acoustic Theory for Rigid Porous Materials," NASA TN D-6196, 1971.

[10]Priestly, M. B., *Non-Linear and Non-Stationary Time Series Analysis*, Academic Press, New York, 1989.

[11]Keefe, L. R., Reisenthel, P. H., and Love, J. F., "Time-Domain Nonlinear Characterization of Acoustic Liner Response," NEAR TR 601, Nielsen Engineering & Research, Apr. 2004

[12]Reisenthel, P. H., Pruzan, D. A., Lesieutre, D. J., and Love, J. F., "Nonlinear Characterization of Electromagnetic Pulse Response Using Continuous Wave Electromagnetic Data," NEAR TR 602, Nielsen Engineering & Research, Apr. 2004.

[13]Prazenica, R. J., Reisenthel, P. H., and Kurdila, A. J., "Novel System Identification Tools for Multiresolution Analysis of Aeroservoelastic Flight Test Data," NEAR TR 600, Nielsen Engineering & Research, Jan. 2004.

[14]Chadran, K., Colton, D., Päivärinta, L., and Rundell, W., *An Introduction to Inverse Scattering and Inverse Spectral Problems*, SIAM, Philadelphia, PA, 1997.

[15]Hansen, P. C., *Rank-Deficient and Discrete Ill-Posed Problems*, SIAM, Philadelphia, PA, 1998, pp. 362-371.

[16]Kraft, R. E., Yu, J., and Kwan, H. W., "Acoustic Treatment Design Scaling Methods. Volume 2: Advanced Treatment Impedance Models for High Frequency Ranges," NASA/CR-1999-209120/VOL2, Apr. 1999.

[17]McAllister, D. F. and Roulier, J. A., *ACM Transactions on Mathematical Software*, Vol. 7, 1981, pp. 384-386.